Post-packaging frequency tuning of microresonators by pulsed laser deposition

Mu Chiao[1] and Liwei Lin[2]

[1] Department of Mechanical Engineering, The University of British Columbia,
2324 Main Mall, Vancouver, BC, V6T 1Z4, Canada
[2] Berkeley Sensor and Actuator Center, University of California at Berkeley, Berkeley,
CA 94720-1740, USA

E-mail: muchiao@mech.ubc.ca

Abstract
This paper presents a post-packaging tuning process for microresonators by PLD (pulsed laser deposition). The microresonators are first hermetically packaged using a RTP (rapid thermal processing) aluminum-to-silicon nitride bonding process. The resonator mass is then altered by adding materials on the surface of the structure using PLD to achieve the desired resonant frequency. The demonstrated tuning resolution is 0.5% per laser shot with a laser beam spot size of 25×25 μm^2 and fluence of 616 mJ cm^{-2}. The laser pulse duration is 6 ns and a 0.35 μm thick gold film is used as the deposition material for comb-drive microresonators resonating at 12.45 kHz.

1. Introduction

Manufacturing variations in the microfabrication process often result in geometric inconsistency in microdevices. For example, relative tolerance in geometric dimension of microfabricated devices can be as high as $\pm 1/5$ (or $\pm 20\%$) of the minimum feature size [1]. Moreover, due to imperfect ion-reactive etching process, trapezoidal, instead of square shape maybe the true cross section of the micro mechanical beams [2]. As a result, batch-fabricated micro mechanical devices cannot have uniform characteristics. For example, 31 MEMS resonators fabricated on a 4 inch wafer in the Microfabrication Laboratory at UC-Berkeley have been tested with statistical data shown in figure 1. The average natural frequency was 12.42 kHz and the standard deviation was 1.3%.

Post-manufacturing tuning is often needed to obtain uniform properties in the microdevices. Previously, resistive heating and tuning has been applied to piezoresistive pressure sensors to balance the bridge and minimize zero pressure offset [3]. However, the tuning process is often carried out after the devices have been diced and die-attached. For free-standing microstructures such as microresonators, it is preferable to protect the microresonators by bonding a protecting cap wafer to the device wafer prior to any further processing [4].

Furthermore, the reported MEMS resonator tuning process can be divided into two major categories: (1) spring constant tuning and (2) mass tuning. In the first category, either resistive heating [5, 6] or electrostatic force pulling [7] can be used. In the second category, the resonator mass can be modified by localized CVD deposition [8]. However, these methods are difficult to implement in the wafer-level manufacturing process.

This paper presents a novel post-packaging tuning scheme and figure 2 shows the process flow. The new tuning approach uses a post-packaging PLD process that has the advantages of precise process control, versatility and can be easily implemented into the post-packaging process as compared with previously demonstrated methods.

2. Post-packaging PLD tuning process

The schematic diagram of the post-packaging PLD frequency tuning process is illustrated in figure 3. A five-mask surface micromachining process similar to the comb-drive resonator fabrication process [2] is used to fabricate microresonators with integrated sealing rings. As shown in figure 3, LPCVD
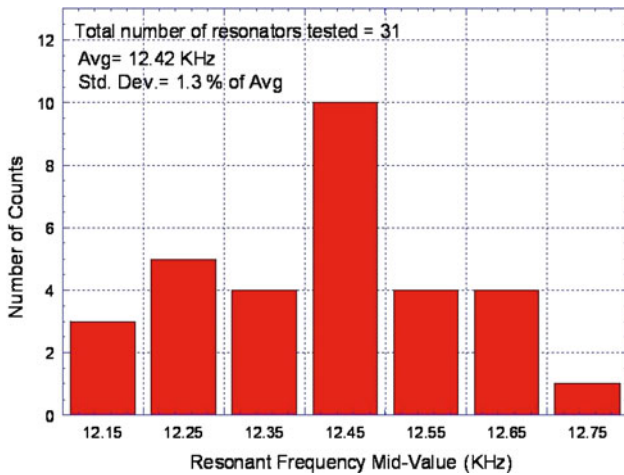
Figure 1. Histogram of resonant frequency of 31 MEMS resonators fabricated at the UCB Microfabrication Laboratory.
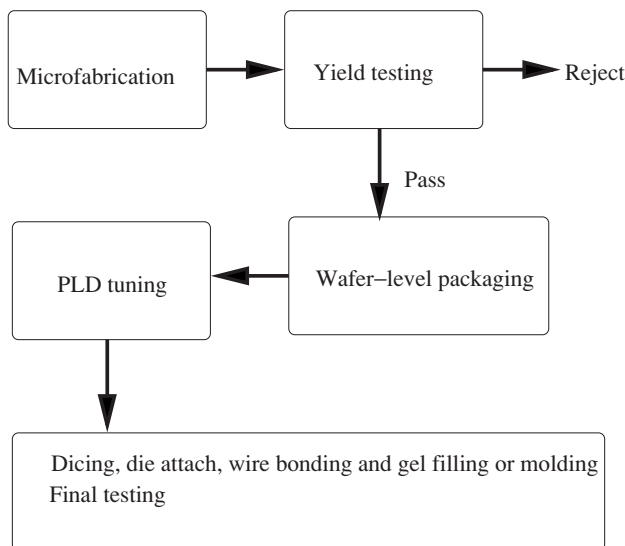

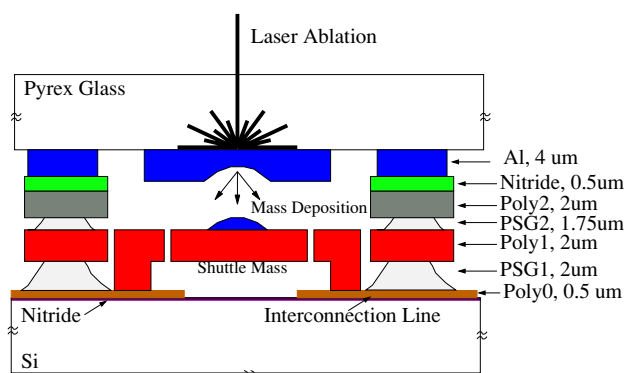**Figure 2.** Packaging and post-packaging PLD tuning process flow.

Figure 3. Schematic diagram showing the post-packaging frequency tuning process by PLD.

low-stress silicon nitride of 3500 Å is deposited as an insulation layer and the ground plan of *in situ* doped polysilicon 0.5 μm thick (poly0) is then deposited using LPCVD and patterned with reactive ion etching (RIE). The sacrificial layer of LPCVD

phosphorous-doped glass (PSG) of 2 μm is deposited and patterned with two masks—dimple and anchor areas using RIE [2]. The structural layer of 2 μm thick undoped polysilicon (poly1) is deposited using LPCVD and RIE-patterned. LPCVD PSG of 1.75 μm (PSG2) is deposited and annealed at 1000 °C for 2 h to perform drive-in dopants from PSG into the poly1 layer. Stacking layers of 2 μm thick polysilicon (poly2) and the bonding layer of 0.5 μm thick LPCVD silicon nitride are deposited and patterned. After the microresonators are packaged by a RTP wafer bonding process [9], the resonant frequency is measured subsequently and frequency tuning range is calculated. A pulsed laser (532 nm, 0.6 mJ and 6 ns pulse duration) with a variable energy attenuator [10] is introduced to locally sputter the donor metal film that has been pre-deposited on the glass (Pyrex 7740) packaging cap. A shuttle plate is designed as part of the resonator to allow re-deposition of the donor metal such that a reduction in resonant frequency is expected. Since PLD tuning always adds mass to the target surface, the microresonators can be designed to have a higher natural frequency that can be tuned down to meet the specification.

Due to the time (ns) and length scale (sub-μm to μm) encountered in this experiment, the heat transfer problem in the PLD process can be modeled by the *Fourier* law [11]. Therefore, thickness and thermal diffusion length of the donor film dominate the PLD process and can be categorized into two regimes [12]:

(1) *Thick film*. Film thickness much larger than the thermal diffusion length $\sqrt{\alpha \Delta t}$ (α and Δt are the thermal diffusivity of the donor film and the pulsed laser duration, respectively).

(2) *Thin film*. Film thickness much smaller than $\sqrt{\alpha \Delta t}$.

In the *thick film* regime, as illustrated in figure 4, under high intensity and short pulse laser irradiation, the thermal energy is absorbed within the first few nanometers of the donor film [13] before the heat spreads out. As a result, nonuniform heating occurs and the metal vapor can build up at the metal film–glass interface [14, 15] and push the rest of the film out. Two time constants affect the PLD event: (1) the time required for melt-through of the whole film thickness (t_b) and (2) the time required for the onset of vaporization at the film–substrate interface (t_v). t_b and t_v are functions of donor film thickness, laser fluence (energy per unit area) and laser duration. Qualitatively, for thinner films and lower laser fluence with longer laser duration, the film melts through before vaporization occurs ($t_b < t_v$). In this case, liquid metal is then pushed off by the vapor pressure built up at the film–substrate interface. On the other hand, for thicker films and higher laser fluence with shorter laser duration, vaporization could occur before melt-through of the entire film ($t_b > t_v$). As such, a burst phenomenon occurs when the trapped, super-heated vapor at the film–substrate interface initiates a crack in the film and rips off the rest of the solid layer [14].

In the *thin film regime*, the donor film has a thickness much less than its thermal diffusion length and uniform heating is a reasonable assumption. The PLD process can be modeled as the film is heated uniformly above the boiling temperature [15]. Evaporation of the donor film and subsequent condensation on the accepting substrate complete the PLD process. The
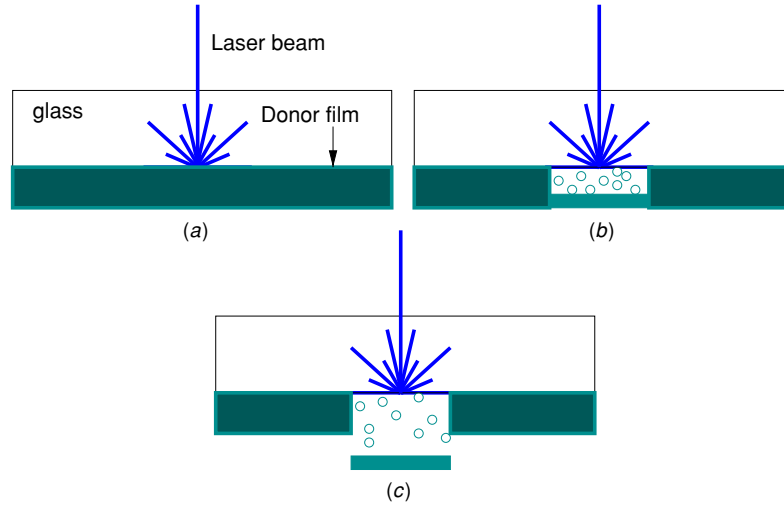
Figure 4. PLD mechanism for film thickness much larger than its thermal diffusion length ($\sqrt{\alpha \Delta t}$). (a) Laser irradiation begins, (b) vapor builds up at interface and (c) vapor pushes film out.

Table 1. Threshold fluences, E_v, for donor films of In, Al and Au of different thickness.

	Thickness (μm)	$\sqrt{\alpha t}$ (μm)	E_v (mJ cm^{-2}) Experimental	E_v Theoretical
Film thickness $\gg \sqrt{\alpha t}$ Thick film	In (4)	0.5	950	–
	Al (4)	0.7	1620	–
Film thickness $\ll \sqrt{\alpha t}$ Thin film	Cr/Au (0.02/0.35)	0.9	587	618

heat transfer process can be simplified if the heat loss to the glass substrate is neglected and the laser irradiation can be approximated as a uniform heat source generated within the thin film [15]. The heat transfer process can be modeled by the governing equation and the initial condition as follows [16]:

$$\rho c_p \frac{\partial T}{\partial t} = \dot{q} \qquad T(t = 0) = T_0 \qquad (1)$$

where ρ (kg m^{-3}) and c_p (J kg^{-1} °C^{-1}) are the film density and specific heat in the solid state, respectively, $\dot{q}$ (W m^{-3}) is the heat generation rate per unit volume from the laser irradiation and T_0 (°C) is the initial temperature. In order to have a well-controlled PLD process, it is important to characterize *threshold fluence* E_v, the minimum laser fluence to initiate the PLD process. E_v is calculated by estimating the fluence needed to convert solid metal films into vapor. Assuming 100% energy transfer rate from absorbed laser energy to thermal energy, the heat generation rate per unit volume $\dot{q}$ in the donor film can be written as

$$\dot{q} = \frac{E_s(1 - R)}{\Delta t \, h} \qquad (2)$$

where E_s (J m^{-2}) is the laser fluence. Δt (s) and h (m) are the laser pulse duration and the film thickness, respectively. R is the reflectivity of the metal film at 532 nm wavelength. Therefore, E_s can be found as a function of T by solving equations (1) and (2),

$$E_s = \rho c_p (T - T_0) \frac{h}{1 - R}. \qquad (3)$$

Table 2. Material properties of gold [18, 19].

	Symbol	Value	Unit
Density	ρ	19 300	kg m^{-3}
Thermal diffusivity	α	123×10^6	m^2 s^{-1}
Thermal conductivity	k	311	W m^{-1} °C^{-1}
Latent heat	H	1110×10^6	J m^{-3}
Specific heat (solid)	c_p	131	J kg^{-1} °C^{-1}
Specific heat (liquid)	c_{pl}	2.75×10^6	J m^{-3} °C^{-1}
Boiling temperature	T_v	2877	°C
Melting temperature	T_m	1063	°C
Reflectivity	R	0.5	–

The minimum laser fluence E_v can then be derived as [17]

$$E_v = E_s + \frac{Hh}{1 - R} + \frac{c_{pl}(T_v - T_m)h}{1 - R}$$
$$= \rho c_p(T_m - T_0)\frac{h}{1 - R} + \frac{Hh}{1 - R} + \frac{c_{pl}(T_v - T_m)h}{1 - R} \qquad (4)$$

where H (J m^{-3}) is the latent heat of the film, c_{pl} (J m^{-3} °C) is the specific heat of the molten film, T_v and T_m are the film boiling and melting temperatures, respectively. E_v calculated from equation (4) for Cr/Au thin film is summarized in table 1. Assuming that the film temperature reaches a maximum at the end of irradiation ($\Delta t = 6$ ns), E_v is calculated as 618 mJ cm^{-2} for gold films (of 0.35 μm in thickness). The physical properties used in the calculation are summarized in table 2 [18, 19].

3. Experimental results

Threshold fluence, E_v, for three experimental donor materials, indium, aluminum and gold, of different thickness is
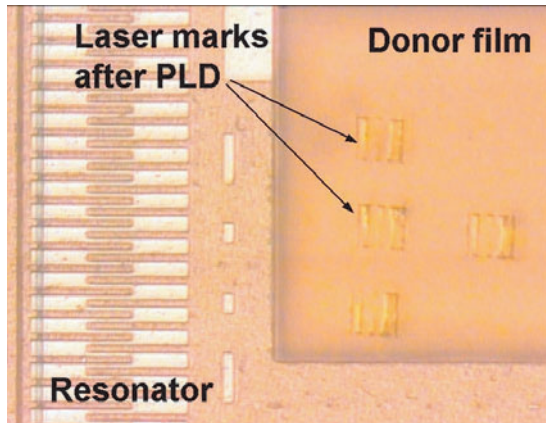
Figure 5. Optical microphoto of the post-packaging PLD results (see-through glass packaging cap).
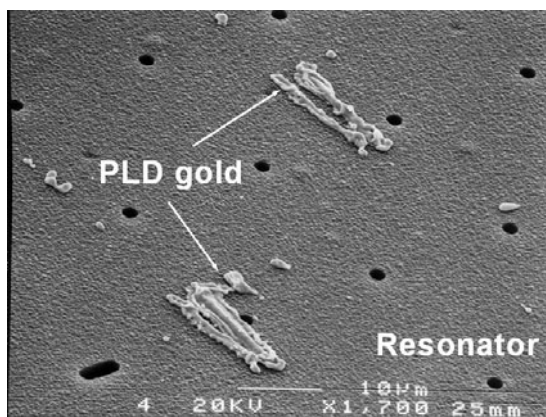

Figure 6. Close-up view at the center of the micro resonator showing two big PLD gold pieces from two laser shots.

Figure 7. SEM microphoto of the donor film being partially removed by the laser beam.

Figure 8. Spectrum measured by a microstroboscope of a resonator before and after the PLD frequency tuning process.

Figure 9. Schematic diagram of an undamped spring–mass system with mass deposition (Δm).

characterized experimentally with visual inspections. The results are summarized in table 1. Experimentally, the laser fluence is gradually increased until a substantial amount of film that can be identified under an optical microscope is deposited onto the accepting substrate. As shown in table 1, for the case of *thin film*, a 4.9% discrepancy between theoretical and experimental results exists and that could be from visual measurement errors, material properties and the fact that additional Cr (200 Å) is used as an adhesion layer for Au.

Figure 5 shows the top view of the PLD tuning results. After four pulsed laser shots are introduced (fluence = 616 mJ cm^{-2}), four laser marks in the donor film (Cr/Au, 200/3500 Å) can be identified through the Pyrex glass packaging cap and the microresonator remains structurally sound. Figure 6 shows the SEM microphoto of a close-up look at a microresonator surface after post-packaging PLD tuning process. The glass packaging cap has been forcibly removed and the PLD gold beads can be identified on the resonator surface as the result of two laser shots at two different locations. The laser beam size and fluence used were 25 × 25 μm^2 and 616 mJ cm^{-2}, respectively. On the glass side, as shown in figure 7, the donor film has been partially removed by the laser power. The irregular shape could be the result of the non-uniformity distribution of the laser intensity in the
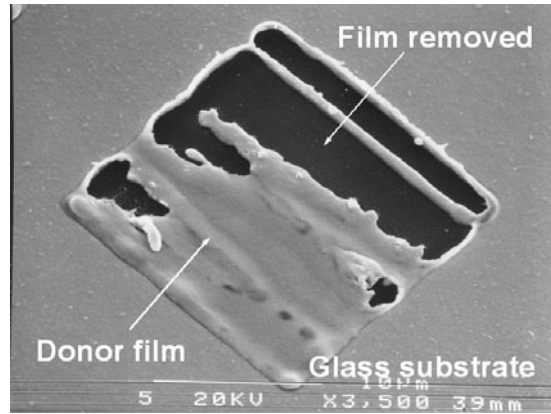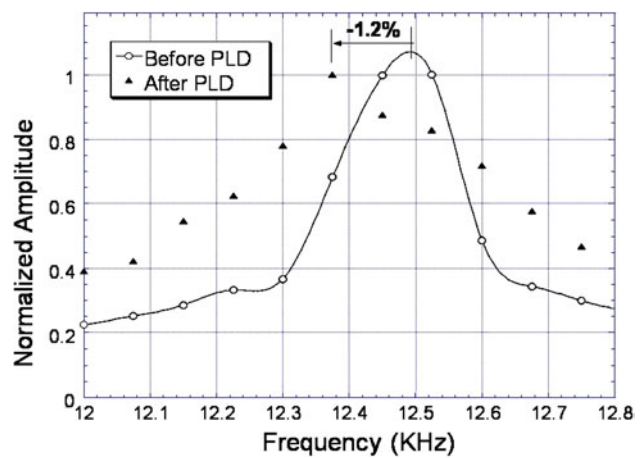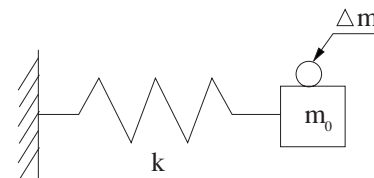
beam profile. Figure 8 shows the measured spectrum of a resonator before and after the PLD tuning process and −1.2% of frequency change is observed. The measurement resolution is 80 Hz and the measurement is performed in air. In this case, aluminum donor film of 4 μm in thickness was used and the applied laser fluence was 1860 mJ cm^{-2}. The resonator did not go through the RTP process and the PLD process was conducted by placing and aligning a donor-film wafer on top of the resonator. It is observed that the quality factor decreases after the PLD deposition process as shown in figure 8, and part of the reason could be from the extra deposition of mass that contributes more air damping effect.

The change in resonant frequency may be modeled by an undamped spring–mass model, as shown in figure 9. The natural frequency of a mass–spring system can be
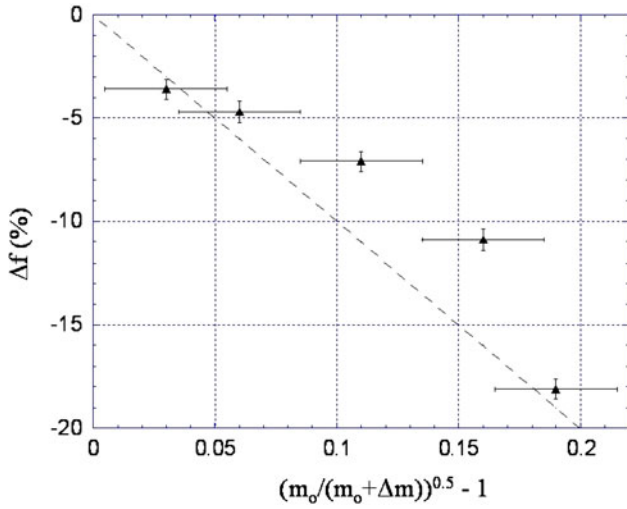
Figure 10. Experimental results showing a frequency shift (Δf, in %) with respect to $(m_0/(m_0 + \Delta m))^{0.5} - 1$ and compared to theoretical prediction by equation (7) (dashed line).

derived as

$$f = \frac{1}{2\pi}\sqrt{\frac{k}{m}} \quad (5)$$

where k and m are the spring constant and mass of the resonator, respectively. Any additional mass deposited (Δm) would result in a natural frequency reduction. The frequency change, Δf, can be defined as

$$\Delta f = \frac{f - f_0}{f_0} \quad (6)$$

$$= \left(\sqrt{\frac{m_0}{m_0 + \Delta m}} - 1\right) \quad (7)$$

where f_0 and f are the natural frequency before and after the PLD process, respectively. m_0 is the resonator mass before the PLD process and is calculated using the comb-resonator layout and thickness of the polysilicon structural layer. Experimentally, indium donor film of 4 μm in thickness was used and Δm was controlled by using multiple laser shots. Δm is estimated using image processing software to measure the size of the deposition area and SEM microphotos to estimate the deposition thickness. The experimental results of Δf versus $\sqrt{\frac{m_0}{m_0 + \Delta m}} - 1$ are shown in figure 10. The error bars are estimated according to the confidence level of the area measured by the image processing software under an optical microscope. The theoretical prediction according to equation (7) is plotted in figure 10 and the mismatch between experimental results and theoretical prediction could result from the misestimation of deposited film thickness under the SEM due to viewing angle and the surface topography of the deposited film.

In order to demonstrate the controllability of the PLD tuning process, a variable number of laser shots with fixed beam size and fluence is conducted on the donor film for each resonator. The resonator frequency is measured before and after the PLD process and frequency changes (Δf) are recorded and correlated to the number of laser shots. It is assumed that the mass deposition, Δm, is proportional to the
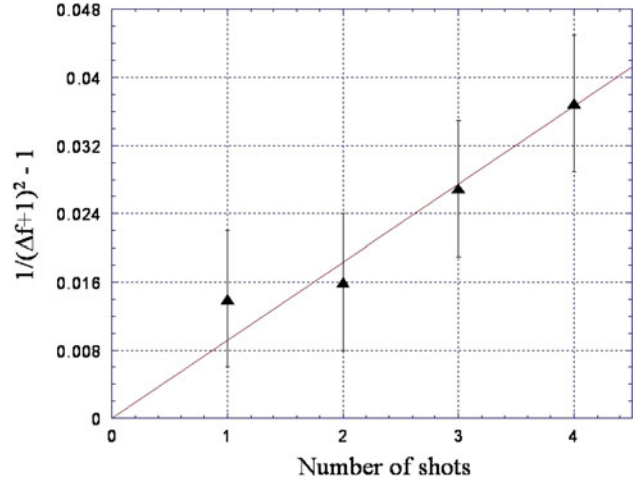
Figure 11. Experimental results showing linear correspondence of the frequency shift (Δf, in %) with respect to the number of laser shots.

number of laser shots. Following equation (7), the number of shots can be related to Δf as

$$(\Delta f + 1)^2 = \frac{m_0}{m_0 + \Delta m} \quad (8)$$

$$\frac{1}{(\Delta f + 1)^2} - 1 \sim \Delta m \sim \text{Number of laser shots.} \quad (9)$$

Experimental results shown in figure 11 confirm the theoretical prediction, where a pulsed laser with a beam size of 25×25 μm^2 and fluence of 616 mJ cm^{-2} was used. Gold of 0.35 μm with a thin Cr (200 Å) adhesion layer was used as the donor film. Four resonators were investigated and the resonant frequencies were measured before and after the PLD process. As extracted from figure 11, the Δf corresponding to 1, 2, 3 and 4 laser shots are 0.7, 0.8, 1.3 and 1.8%, respectively and the average resolution of the tuning process is 0.5% per laser shots. The error bars are determined from the confidence level of resonant frequency estimation using optical measurement.

4. Conclusion and discussion

In this paper, a post-packaging frequency tuning technique by PLD has been demonstrated by using gold, indium or aluminum as the donor material. The spectrum of a MEMS resonator is measured before and after the PLD frequency tuning process and a frequency reduction of 1.2% is demonstrated. The frequency change is measured as a function of the deposited donor mass and a linear relation was predicted by an undamped spring–mass vibration model and experimentally verified. The threshold fluence E_v has been characterized theoretically for *thin films* and compared with experimental results. For *thick films*, the experimental characterization has been presented. The controllability of the PLD tuning process has been demonstrated as the frequency change is directly related to the number of laser shots and the tuning resolution was demonstrated as 0.5% per laser shot with

a laser beam size of $25 \times 25 \ \mu m^2$. The tuning resolution can be significantly improved by using thinner donor metal film and smaller laser beam size.

Although slight quality factor (Q) degradation of hermetically-packaged microresonators was observed after the PLD process, a vacuum-packaged resonator might see less degradation of Q due to the surface roughness of the deposited mass. This problem could be minimized by introducing a second laser through the transparent glass area cleared by the first PLD laser. The second pulsed laser could be used to locally melt and re-shape the deposited donor film and the surface roughness can be minimized.

The choice of donor films could assert significant effects in the PLD tuning process. In order to demonstrate this proof-of-concept work, we have chosen heavier metals such as gold as the main donor film such that the frequency change can be easily identified. In general, by using the current optical measurement method, it has been observed in our experiments that Cr/Au donor film results in more noticeable change in resonant frequency over other materials such as Al and In of the same thickness. Possibly due to the greater density of the Cr/Au film compared to Al and In. However, if fine tuning is needed, donor films with smaller density may be preferable.

Acknowledgments

References

[1] Madou M 2002 *Fundamentals of Microfabrication* 2nd edn (Boca Raton, FL: CRC Press)

[2] Tang W, Nguyen T, Judy M and Howe R 1990 Electrostatic-comb drive of lateral polysilicon resonators *Sensors and Actuators* A **21** 328–31

[3] Feldbaumer D and Babcock J 1995 Theory and application of polysilicon resistor trimming *Solid-State Electron.* **38** 1861–9

[4] Chiao M and Lin L 2004 Sealing technologies *MEMS Packaging* ed T-R Hsu (London: IEE) chapter 3 pp 61–83

[5] Wang K, Wong A C, Hsu W T and Nguyen C T-C 1997 Frequency trimming and Q-factor enhancement of micromechanical resonators via localized filament annealing *Transducers'97* pp 109–12

[6] Remtema T and Lin L 2000 Active frequency tuning for microresonators by localized thermal stressing effects *Technical Digest of Solid-State Sensor and Actuator Workshop* pp 363–6

[7] Lee K B and Cho Y H 1997 Frequency tuning of a laterally driven microresonator using an electrostatic comb array of linearly varied length *Transducers'97* pp 113–6

[8] Joachim D and Lin L 1999 Localized deposition of polysilicon for MEMS post-fabrication processing *Proc. ASME Int. Mechanical Engineering Congress and Exposition—MEMS* pp 37–42

[9] Chiao M and Lin L 2001 Accelerated hermeticity testing of a glass–silicon package formed by RTP aluminum-to-silicon nitride bonding *11th Int. Conference on Solid-State Sensors and Actuators, Transducers'01, Technical Digest (Munich, Germany)* pp 190–3

[10] New Wave Research 47613 Warm Springs Blvd. Fremont, CA 94539, USA

[11] Majumdar A 1993 Microscale heat conduction in dielectric thin films *Trans. ASME—J. Heat Transfer* **115** 7–16

[12] Bohandy J, Kim B F, Adrian F J and Jette A N 1988 Metal deposition at 532 nm using a laser transfer technique *J. Appl. Phys.* **63** 1158–62

[13] Siegel R and Howell J R 1992 *Thermal Radiation Heat Transfer* 3rd edn (Chichester: Taylor and Francis)

[14] Schultze V and Wagner M 1991 Blow-off of aluminum films *Appl. Phys.* A **53** 241–8

[15] Baseman R J, Froberg N M, Andreshak J C and Schlesinger Z 1990 Minimum fluence for laser blow-off of thin gold films at 248 and 532 nm *Appl. Phys. Lett.* **56** 1412–4

[16] Holman J 1992 *Heat Transfer* 7th edn (New York: McGraw-Hill)

[17] Toet D, Smith P and Sigmon T 2000 Experimental and numerical investigations of a hydrogen-assisted laser-induced materials transfer procedure *J. Appl. Phys.* **87** 3537–46

[18] Grigoriev I and Meilikhov E (ed) 1997 *Handbook of Physical Quantities* 1st edn (Boca Raton, FL: CRC Press)

[19] Gray D (ed) 1972 *American Institute of Physics Handbook* 3rd edn (New York: American Institute of Physics)